PHYSICAL REVIEW D **78,** 054503 (2008)

Series expansions of the density of states in $SU(2)$ lattice gauge theory

A. Denbleyker,* Daping Du,+ Yuzhi Liu,‡ and Y. Meurice§
Department of Physics and Astronomy, The University of Iowa, Iowa City, Iowa 52242, USA

A. Velytsky‖
Enrico Fermi Institute, University of Chicago, 5640 South Ellis Avenue, Chicago, Illinois 60637, USA, and HEP Division and Physics Division, Argonne National Laboratory, 9700 Cass Avenue, Argonne, Illinois 60439, USA
(Received 24 July 2008; published 8 September 2008)

We calculate numerically the density of states $n(S)$ for $SU(2)$ lattice gauge theory on L^4 lattices [S is the Wilson's action and $n(S)$ measures the relative number of ways S can be obtained]. Small volume dependences are resolved for small values of S. We compare $\ln(n(S))$ with weak and strong coupling expansions. Intermediate order expansions show a good overlap for values of S corresponding to the crossover. We relate the convergence of these expansions to those of the average plaquette. We show that, when known logarithmic singularities are subtracted from $\ln(n(S))$, expansions in Legendre polynomials appear to converge and could be suitable to determine the Fisher's zeros of the partition function.

DOI: 10.1103/PhysRevD.78.054503 PACS numbers: 11.15.Ha, 11.15.−q, 11.15.Me, 12.38.Bx

I. INTRODUCTION

Quantum chromodynamics is a widely accepted theory of strong interactions. From a theoretical point of view, understanding the large distance behavior in terms of the weakly coupled short distance theory has been an important challenge. The connection between the two regimes can be addressed meaningfully using the lattice formulation. In the pure gauge theory (no quarks) described with the standard Wilson's action, no phase transition between the weak and strong coupling regimes has been found numerically for $SU(2)$ or $SU(3)$, and the theory should be in the confining phase for all values of the coupling. Recently, convincing arguments have been given [1,2] in favor of the smoothness of the renormalization group flows between the two fixed points of interest, putting the confining picture on more solid mathematical ground.

The absence of phase transition discussed above suggests that it is possible to match the weak coupling and the strong coupling expansions of the lattice formulation. However, if we consider these two expansions, for instance, for the average $SU(2)$ plaquette as a function of $\beta = 4/g^2$, we see in Fig. 1 that there is a crossover region (approximately $1.5 < \beta < 2.5$) where neither of the two expansions seem to work. This behavior is probably related to singularities in the complex β plane [3,4] that are not completely understood. In the case of the one plaquette model [5], taking the inverse Laplace transform with respect to β (Borel transform) of the partition function yields a function that has better convergence properties. It would be interesting to know if this feature persists on $V = L^4$ lattices.

In this article, we study expansions of the inverse Laplace transform of the partition function (the density of states) of $SU(2)$ lattice gauge theory on symmetric four-dimensional lattices. The density of states is denoted $n(S)$ and defined precisely in Sec. II. It gives a relative measure of the number of ways to get a value S of the action. Knowing $n(S)$, we can calculate the partition function and its derivatives for any real or complex value of β. In particular, it could be used to determine the Fisher's zeros

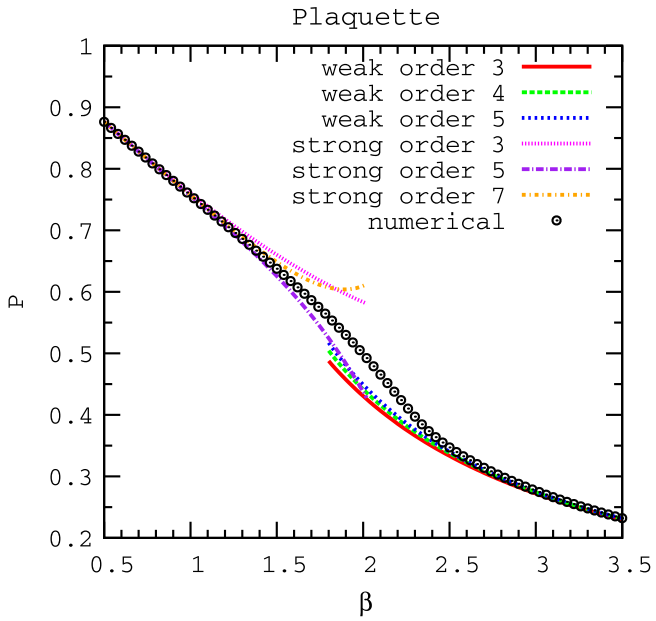

FIG. 1 (color online). Weak and strong coupling expansions of the average plaquette P for $SU(2)$ at various orders in the weak and strong coupling expansions compared to the numerical values.

*alan-denbleyker@uiowa.edu
+daping-du@uiowa.edu
‡yuzhi-liu@uiowa.edu
§yannick-meurice@uiowa.edu
‖vel@theory.uchicago.edu

of the partition function [6–8]. The choice of $SU(2)$ is motivated by the existence of a particular symmetry [9] which allows one to determine the behavior of $n(S)$ near its maximal argument without extra calculation. In Sec. III, we explain why $\ln(n(S))$ is expected to scale like the volume and can be interpreted as a "color entropy." Numerical calculations of $n(S)$ obtained by patching plaquette distributions multiplied by the inverse Boltzmann weight at values of β increasing by a small increment are presented in Sec. IV. The article is focused on comparisons with numerical data on a 6^4 lattice where finite volume effects are not too large and plaquette distributions broad enough to allow a smooth patching. The values of $n(S)$ on such a lattice are compared with those on a 4^4 and 8^4 lattice. It is interesting to note that the volume dependence is resolvable only for small values of S where a behavior $\ln(S)/V$ is observed for $\ln(n(S))$.

The numerical results are compared with expansions that can be obtained from the strong (Sec. V) and weak (Sec. VI) coupling expansions of the average plaquette. Intermediate orders in these expansions show a good overlap for values of S that correspond to the crossover. We then show that the convergence of the new series can be related empirically to those of the series for the average plaquette. The weak coupling expansion determines the logarithmic singularities of $\ln(n(S))$ at both boundaries. When these singularities are subtracted we obtain a bell-shaped function that can be approximated very well by Legendre polynomials (Sec. VII). We conclude with possible applications for the calculations of the Fisher's zeros and open problems.

II. THE DENSITY OF STATES

We consider the standard pure gauge partition function

$$Z = \prod_l \int dU_l e^{-\beta \mathcal{S}}, \tag{1}$$

with the Wilson action

$$\mathcal{S} = \sum_p (1 - (1/N)\mathrm{Re}\,\mathrm{Tr}(U_p)) \tag{2}$$

and $\beta \equiv 2N/g^2$. We use a D-dimensional cubic lattice with periodic boundary conditions. For a symmetric lattice with L^D sites, the number of plaquettes is

$$\mathcal{N}_p \equiv L^D D(D-1)/2. \tag{3}$$

In the following, we restrict the discussion to the group $SU(2)$ and $D = 4$. For $SU(2)$, one can show [9] that the maximal value of $\mathcal{S}$ is $2\mathcal{N}_p$. We define the average plaquette:

$$P \equiv \langle \mathcal{S}/\mathcal{N}_p \rangle = -d(\ln Z/\mathcal{N}_p)/d\beta. \tag{4}$$

Inserting 1 as the integral of delta function over the numerical values S of $\mathcal{S}$ in Z, we can write

$$Z = \int_0^{2\mathcal{N}_p} dS n(S) e^{-\beta S}, \tag{5}$$

with

$$n(S) = \prod_l \int dU_l \delta\Big(S - \sum_p (1 - (1/N)\mathrm{Re}\,\mathrm{Tr}(U_p))\Big). \tag{6}$$

We call $n(S)$ the density of states. A more general discussion for spin models [10] or gauge theories [11] can be found in the literature where the density of states is sometimes called the spectral density. From its definition, it is clear that $n(S)$ is positive. Assuming that the Haar measure for the links is normalized to 1, the partition function at $\beta = 0$ is 1, and consequently we can normalize $n(S)$ as a probability density.

A first idea regarding the convergence properties of various expansions can be obtained from the single plaquette model [5]. In that case, we have

$$n_{1\mathrm{pl}}(S) = \frac{2}{\pi}\sqrt{S(2-S)}. \tag{7}$$

The large β behavior of the partition function is determined by the behavior of $n(S)$ near $S = 0$. In this example, $n(S) \propto \sqrt{S}$ for small S implies that $Z \propto \beta^{-3/2}$ at leading order. Successive subleading corrections can be calculated by expanding the remaining factor $\sqrt{2-S}$ in powers of S and integrating over S from 0 to ∞. If we factor out the leading behavior, we obtain a power series in $1/\beta$. The large order behavior of this power series is determined by the large order behavior of the expansion of $\sqrt{2-S}$, itself dictated by the branch cut at $S = 2$. One can see [5] that the S integration over the *whole* positive real axis converts an expansion with a finite radius of convergence into one with a zero radius of convergence. On the other hand, if the S integration is carried over the interval $[0, 2]$, the resulting series converges but the coefficients need to be expressed in terms of the incomplete gamma function. From this example, one may believe that it is easier to approximate $n(S)$ than the corresponding partition function. However, it is not clear that these considerations will survive the infinite volume limit. Note also that the behavior of $n(S)$ near $S = 2$ can be probed by taking $\beta \to -\infty$ in agreement with the common wisdom that the large order behavior of weak coupling series can be understood in terms of the behavior at small negative coupling.

It was shown [9] that, if the lattice has an even number of sites in each direction and if the gauge group contains $-\mathbb{1}$, it is possible to change $\beta\mathrm{Re}\,\mathrm{Tr}U_p$ into $-\beta\mathrm{Re}\,\mathrm{Tr}U_p$ by a change of variables $U_l \to -U_l$ on a set of links such that for any plaquette exactly one link of the set belongs to that plaquette. This implies that

$$Z(-\beta) = e^{2\beta\mathcal{N}_p} Z(\beta). \tag{8}$$

This symmetry implies that

$$n(2\mathcal{N}_p - S) = n(S). \tag{9}$$

In the following, we will be working exclusively with $SU(2)$ which contains $-\mathbb{1}$ and lattices with even numbers of sites in every direction. We will thus assume that Eq. (9) is satisfied and we need only to know $n(S)$ for $0 \leq S \leq \mathcal{N}_p$.

III. VOLUME DEPENDENCE

In this section, we discuss the volume dependence of the density of state. We make this dependence explicit by writing $n(S, \mathcal{N}_p)$. Given the density of states, we can always write

$$f(x, \mathcal{N}_p) \equiv \ln(n(x\mathcal{N}_p, \mathcal{N}_p))/\mathcal{N}_p. \tag{10}$$

The function is nonzero only if $0 \leq x \leq 2$. The symmetry (9) implies that

$$f(x, \mathcal{N}_p) = f(2 - x, \mathcal{N}_p). \tag{11}$$

In the statistical mechanics interpretation of the partition function (where β is an inverse temperature), $f(x, \mathcal{N}_p)$ can be interpreted as a density of entropy. The existence of the infinite volume limit requires that

$$\lim_{\mathcal{N}_p \to \infty} f(x, \mathcal{N}_p) = f(x), \tag{12}$$

with $f(x)$ volume independent. In the same limit, the integral (5) can be evaluated by the saddle point method. The maximization of the integrand requires

$$f'(x) = \beta. \tag{13}$$

We believe that $f(x)$ is strictly increasing for $0 < x < 1$ with an absolute maximum at $x = 1$. By symmetry, this would imply that $f(x)$ is strictly decreasing for $1 < x < 2$. We also believe that $f'(x)$ is strictly decreasing and that Eq. (13) has a unique solution (with positive β if $0 < x < 1$ and negative β if $1 < x < 2$). The numerical study of Sec. IV is in agreement with these statements, but we are not aware of mathematical proofs. Assuming that Eq. (13) has a unique solution, the infinite volume solution should be $x = P$, the average plaquette defined above. We can then convert an expansion for P into an expansion of f. If we want to include the volume dependence, the distribution has a finite width, and we should expand about the saddle point and perform the integration. In the following, we will work at large but finite volume, and residual volume dependence in f will be kept implicit in equations.

The behavior of $f(x)$ for small x can be probed by studying the model at large positive β (weak coupling expansion discussed in Sec. VI). On the other hand, at small values of β (strong coupling expansion discussed in Sec. V), the partition function is dominated by the behavior of $f(x)$ near its peak value $x = 1$. For convenience, we introduce notations suitable for the study of the density of state near $x = 1$:

$$g(y) \equiv f(1 + y). \tag{14}$$

$g(y)$ is then an even function defined for $-1 < y < 1$.

IV. NUMERICAL CALCULATION OF $n(S)$

To find $n(S)$ numerically we will use a Monte Carlo simulation to create configurations of $SU(2)$ for different values of β. In the following example we will follow the steps we will use to find $n(S)$ for a volume of 6^4. We will start with 550 different sets of data ranging from $\beta = 0.02$ to $\beta = 11.00$ in steps of 0.02 and with sizes of 10^5 con-

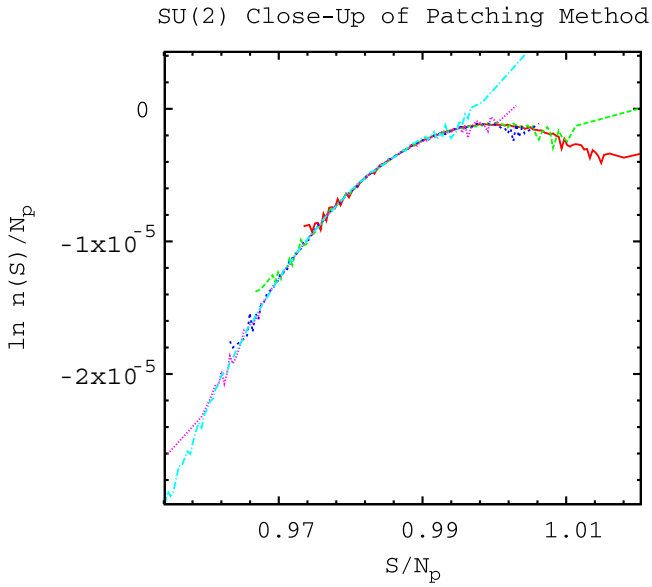

FIG. 2 (color online). Close-up of the patching process for 6^4.

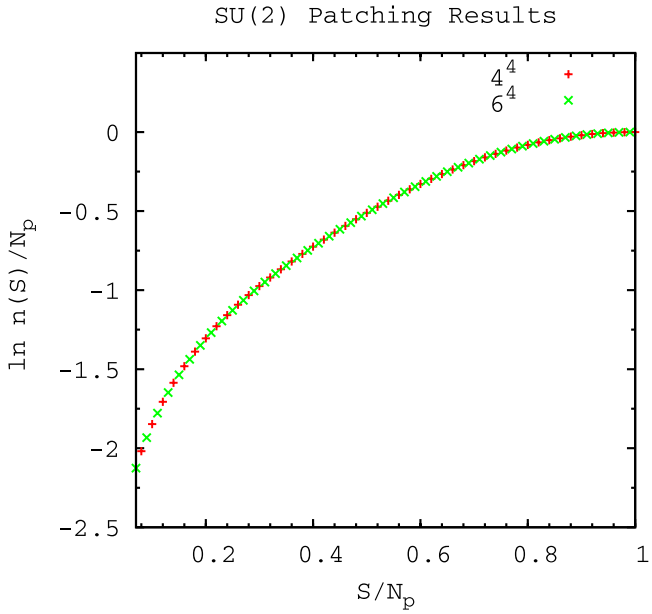

FIG. 3 (color online). Results of patching for 4^4 and 6^4.

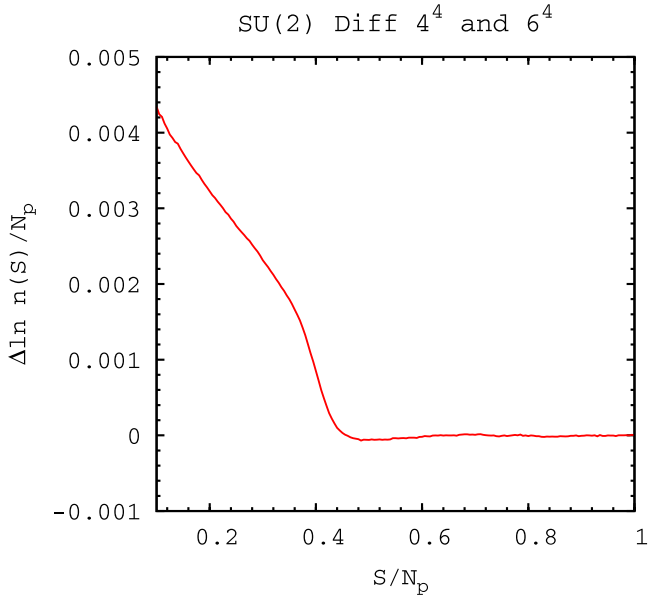

FIG. 4 (color online). The difference between $\ln(n(S))/\mathcal{N}_p$ for 4^4 and 6^4.

figurations. To join the data from different values of β we will first create histograms of each set of data; each of these histograms is roughly Gaussian in shape. We then filter out the data that have statistics that are lower than half of the maximum bin. We can then remove the beta dependence by multiplying the height of each bin by $e^{\beta S}$. We will be left with a series of arches which when overlaid on each other form the curve $n(s)$. To create this overlay we will start with the lowest β, which will correspond to the peak of $n(s)$, and then take the logarithm of this. We will then look at the neighboring β and do the same thing but then shift it

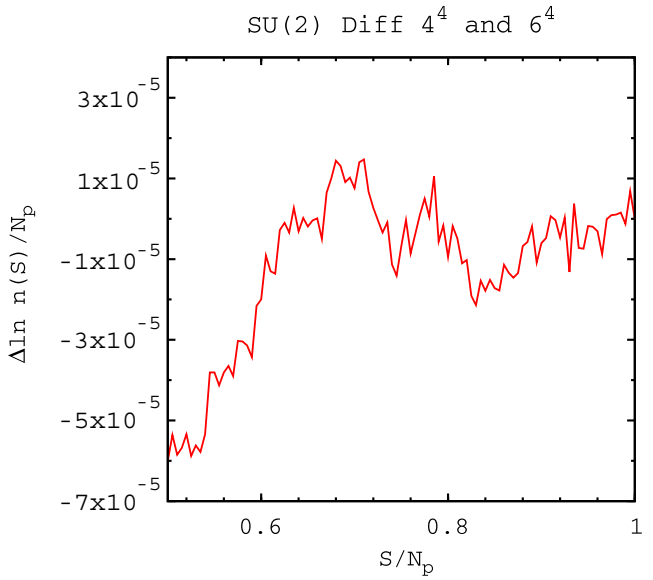

FIG. 5 (color online). The difference between $\ln(n(S))/\mathcal{N}_p$ for 4^4 and 6^4 with $\beta > 0.5$ (close-up).

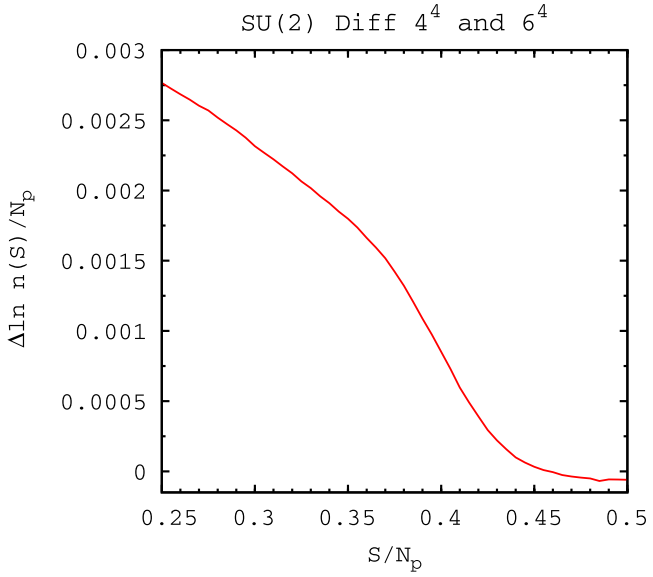

FIG. 6 (color online). The difference between $\ln(n(S))/\mathcal{N}_p$ for 4^4 and 6^4 with $\beta < 0.5$ (close-up).

up or down so that the average distance in the bins overlapping with the first is zero. We will then continue in this manner until the supply of data sets has been exhausted. A portion of this process can be seen in Fig. 2. We then average the points for each bin together and divide both the bin width and height by $\mathcal{N}_p$ and shift the top of the curve to zero to make the final output, which can be seen in Fig. 3 for both 4^4 and 6^4. We see that they overlap well.

We now consider the difference between two different volumes, as shown in Fig. 4. We can see in Fig. 5 that as we get closer to $S/\mathcal{N}_p = 1$ this difference turns into noise, and as we get closer to $S/\mathcal{N}_p = 0$ we see a volume dependence growing. The logarithmic nature of this growth is illustrated in Figs. 6 and 7. The results reported here correspond to the difference between 6^4 and 4^4. We have also studied the difference between 8^4 and 6^4 and found consistent results. Calculation at larger volumes is much more computationally expensive and requires many more sets of data because of the narrow width of the distributions.

V. STRONG COUPLING EXPANSION

In this section, we discuss the strong coupling expansion of the logarithm of the density of state. We will work with the shifted function $g(y)$ defined in Eq. (14). The strong coupling expansion of P can be extracted from the expansion of $\ln Z$ given in Refs. [12,13] using appropriate rescalings (for instance, the β used there is one-half of the β used here). The expansion is of the form

$$P(\beta) \simeq 1 + \sum_{m=1} a_{2m-1}\beta^{2m-1}. \tag{15}$$

The values of the coefficients are given in Table I.

TABLE I. Strong coupling expansion coefficients defined in the text.

m	a_{2m-1}	g_{2m}	h_{2m}
1	$-\frac{1}{4}$	-2	$-\frac{5}{4}$
2	$\frac{1}{96}$	$-\frac{2}{3}$	$-\frac{7}{24}$
3	$-\frac{7}{1536}$	$\frac{20}{9}$	$\frac{89}{36}$
4	$\frac{31}{23\,040}$	$-\frac{16}{45}$	$-\frac{121}{720}$
5	$-\frac{4451}{8\,847\,360}$	$-\frac{16\,816}{2025}$	$-\frac{66\,049}{8100}$
6	$\frac{264\,883}{1\,486\,356\,480}$	$\frac{319\,736}{8505}$	$\frac{2\,566\,393}{68\,040}$
7	$-\frac{403\,651}{5\,945\,425\,920}$	$-\frac{3\,724\,816}{297\,675}$	$-\frac{14\,771\,689}{1\,190\,700}$
8	$\frac{1\,826\,017\,873}{68\,491\,306\,598\,400}$	$-\frac{163\,150\,033}{255\,150}$	$-\frac{2\,610\,017\,803}{4\,082\,400}$

With periodic boundary conditions, the low order coefficients are volume independent. This can be understood from the exact translation invariance for the low order strong coupling graphs that provides a multiplicity that cancels exactly the $1/\mathcal{N}_p$ in Eq. (4). Volume dependence may appear for graphs wrapping around the torus. The simplest such graph is a straight line that closes into itself due to the periodic boundary condition. It appears at order β^{2L} and has a reduced translation multiplicity since translation along the graph does not generate a new graph. This type of graph produces $1/L$ corrections that we have not attempted to resolve here. It would be interesting to understand the connection between such effects and the finite size effects due to wraparound graphs encountered in the transfer matrix formalism (''torelons'') [14].

We will plug the expansion of P in the expansion

$$g(y) \simeq \sum_{m=0} g_{2m} y^{2m}. \tag{16}$$

At lowest order we have $y \simeq a_1\beta$, and the saddle point Eq. (13) yields $2g_2 y \simeq 2g_2 a_1 \beta \simeq \beta$, which implies that $g_2 = 1/(2a_1)$. This procedure can be followed order by order in β. The results are shown in Table I.

Since $n(S)$ is zero for $S = 0$ and $2\mathcal{N}_p$, we expect logarithmic singularities at $x = 0$ and 2 for $f(x)$ and $y = \pm 1$ for $g(y)$. These singularities will cause the strong coupling series to diverge when $|y| \geq 1$. Consequently, we define the subtracted function

$$h(y) \equiv g(y) - A(\ln(1 - y^2)). \tag{17}$$

The coefficient A will be calculated using the weak coupling expansion in Sec. VI. In the infinite volume limit, we have $A = 3/4$. Expanding

$$h(y) \simeq \sum_{m=0} h_{2m} y^{2m}, \tag{18}$$

we obtained coefficients that are shown in Table I for $A = 3/4$. The coefficients g_{2m} and h_{2m} are also shown on a logarithmic scale in Fig. 8. This graph shows that the two types of coefficients become rapidly of the same order,

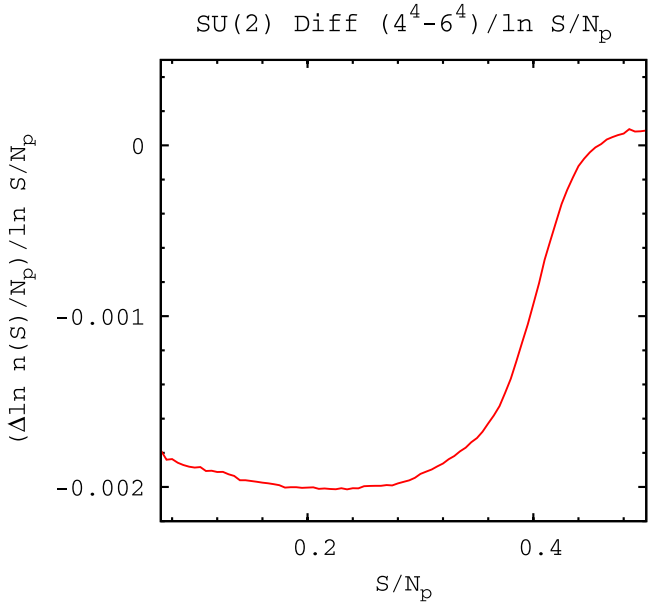

FIG. 7 (color online). The difference between $\ln(n(S))/\mathcal{N}_p$ for 4^4 and 6^4 divided by $\ln(S/\mathcal{N}_p)$.

which indicates singularities in the complex y plane for smaller values of $|y|$ than the ones at ± 1.

In Fig. 9, we show the error made at successive order of the strong coupling expansion of the plaquette. We then show successive approximation of $f(x)$ (Fig. 10) and the corresponding errors (Fig. 11).

We can now compare the apparent convergence of P and f. From Fig. 9 we see that the larger order errors cross

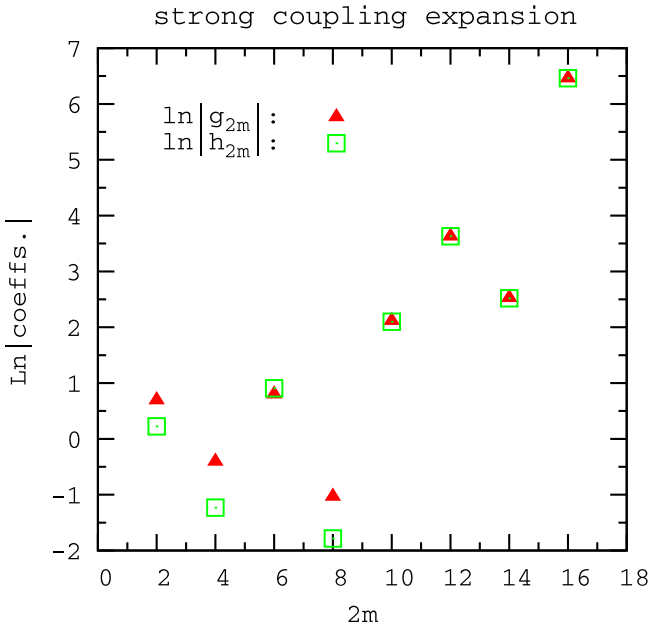

FIG. 8 (color online). Logarithm of the absolute value of g_{2m} and h_{2m}.

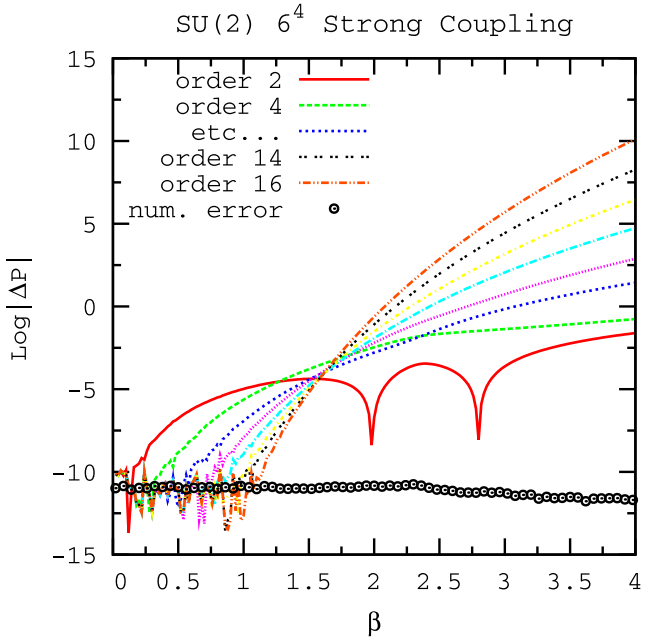

FIG. 9 (color online). Logarithm of the absolute value of the difference between the numerical data and the strong coupling expansion of P at successive orders. For reference, we give the estimated numerical error on P.

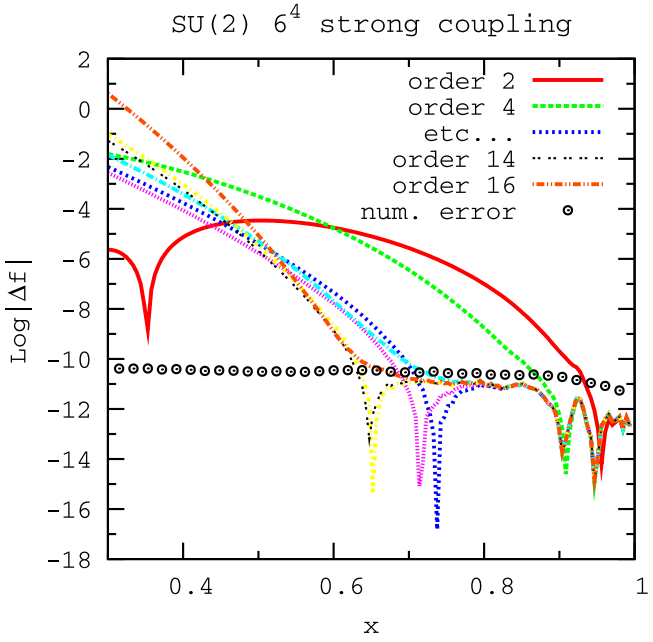

FIG. 11 (color online). Logarithm of the absolute value of the difference between the numerical data and the strong coupling expansion of f at successive orders. For reference, we give the estimated numerical error on f.

between $\beta = 1.5$ and 2. For values of β larger, increasing the order increases the error. This is the sign of a finite radius of convergence [15]. Similarly, the larger order errors for f cross for x between 0.5 and 0.6, which are approximately the values of P in the β interval of crossing. Consequently, it seems like the convergence properties of the two expansions are the same (finite radius of convergence).

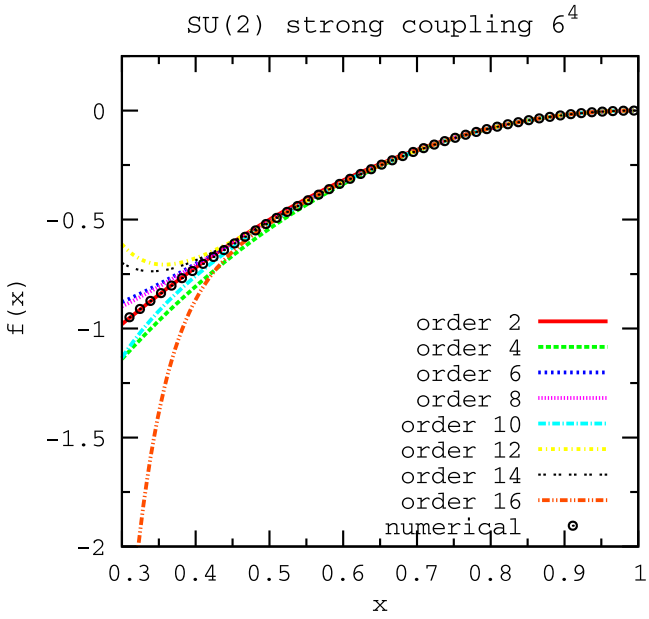

FIG. 10 (color online). Numerical value of $f(x)$ compared to the strong coupling expansion at successive orders.

VI. WEAK COUPLING EXPANSION

In this section, we discuss the weak coupling expansion of $f(x)$. The starting point is the expansion of P in inverse powers of β

$$P(\beta) \simeq \sum_{m=1} b_m \beta^{-m}. \tag{19}$$

We then assume the behavior

$$f(x) \simeq A \ln(x) + \sum_{m=0} f_m x^m. \tag{20}$$

Using the saddle point Eq. (13), and using the leading large β and small x terms, we find

$$\beta \simeq A/x \simeq A/(b_1/\beta), \tag{21}$$

which implies that $A = b_1$ at infinite volume. The procedure can be pursued order by order without difficulty. The result for the two lowest orders is

$$f_1 = b_2/b_1, \qquad f_2 = (b_3 b_1 - b_2^2)/(2b_1^2).$$

Numerical experiments indicate that the two series have the same type of growth (power or factorial). Note that f_0 cannot be fixed by the saddle point equation. The overall height of f depends on the behavior near $x = 1$ [if we insist on normalizing $n(S)$ as the probability density], and it

seems unlikely that it can be found by a weak coupling expansion.

At finite volume, the saddle point calculation of P should be corrected in order to include $1/V$ effects (V the number of sites, L^D for a symmetric lattice). If we perform the Gaussian integration of the quadratic fluctuations, and use the V dependent value of b_1 given in Eq. (23) below, we find after a short calculation that the coefficient A of $\ln(x)$ is

$$A = (3/4) - (5/12)(1/V). \quad (22)$$

This leading coefficient correction predicts a difference of $-0.0013\ln(x)$ for the difference between $f(x)$ for a 4^4 and 6^4 and is roughly consistent with Fig. 7.

Our next task is to find the values of b_m. A closed form expression can be found [16,17] for b_1. For the case $N_c = 2$ and $D = 4$, we obtain

$$b_1 = (3/4)(1 - 1/(3V)). \quad (23)$$

The $(-1/(3V))$ comes from the absence of zero mode $(-1/V)$ in a sum calculated in Ref. [16] plus the contribution of the zero mode with periodic boundary conditions $(+2/(3V))$ calculated in Ref. [17]. Numerical values for b_2 can be found in Ref. [16] and for b_3 in Ref. [18]. In these references, several sums are calculated numerically at particular volumes that do not include 6^4. Rough extrapolations from the existing data indicate that for $V = 6^4$ uncertainties are less than 0.0002 for b_2 and 0.0008 for b_3. For $\beta \geq 3$, these effects are close to the numerical errors for P. In the following, we use the approximate values $b_2 = 0.1511$ and $b_3 = 0.1427$ for $V = 6^4$.

We are not aware of any calculation of b_m for $m \geq 4$ for $SU(2)$. In the case of $SU(3)$, calculations up to order 10 [19] and 16 [20] are available and show remarkable regularities. Using the assumption [3] that $\partial P/\partial\beta$ has a logarithmic singularity in the complex β plane and integrating, we obtained [21] the approximate form

$$\sum_{m=1} b_m \beta^{-k} \approx C(\mathrm{Li}_2(\beta^{-1}/(\beta_m^{-1} + i\Gamma)) + \mathrm{H.c.}), \quad (24)$$

with

TABLE II. Weak coupling coefficients defined in Sec. VI. The choice of b_1 corresponds to $V = 6^4$.

m	b_m	f_m
1	0.7498	0.2015
2	0.1511	0.0999
3	0.1427	0.0796
4	0.1747	0.0791
5	0.2435	0.0908
6	0.368	0.1156
7	0.5884	0.1597
8	0.98	0.2351
9	1.6839	0.3643
10	2.9652	0.5883
11	5.326	0.9828
12	9.7234	1.6883
13	17.995	2.9683
14	33.690	5.3207
15	63.702	9.6945

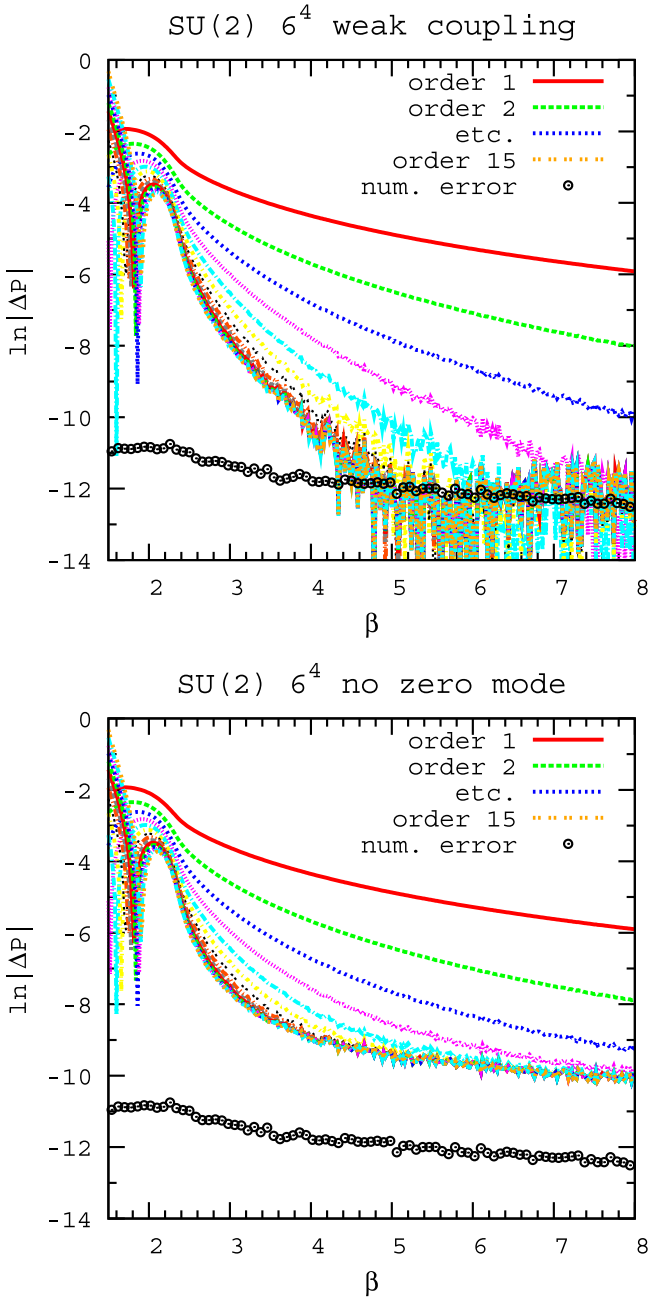

FIG. 12 (color online). Logarithm of the absolute value of the difference between the numerical data and the weak coupling expansion of P at successive orders (above). For reference, we give the estimated numerical error on P. The graph below is the same except that we have not included the zero mode in b_1.

$$\mathrm{Li}_2(x) = \sum_{k=1} x^k/k^2. \tag{25}$$

We believe that at zero temperature, the new parameter Γ which measures the (small) distance from the singularity to the real axis in the $1/\beta$ plane stabilizes at a nonzero value in the infinite volume limit. For reasons not fully understood, this parametrization of the series turns out to work very well for $SU(3)$. For instance, by fixing the value of Γ in the middle of the allowed range and using the values of b_9 and b_{10}, we obtain values of the lower order coefficients with a relative error of 0.2% for b_8 and that increases up to 5% for b_3. In the limit $\Gamma = 0$, the parametrization provides simple predictions for instance $b_3/b_2 \simeq (4/9)\beta_m$. The location of the Fisher's zeros for $SU(2)$ [6] suggests $\beta_m = 2.18$. This implies that $b_3/b_2 \simeq 0.969$ in good agreement with our numerical estimate $b_3/b_2 \simeq 0.944$. In the following we use the values $\beta_m = 2.18$ and $\Gamma = 0.18/\beta_m^2 \simeq 0.038$ (see [6]), and we fixed $C = 0.0062$ in order to reproduce b_3. The numerical values of b_m and the corresponding values of f_m are displayed in Table II.

We have compared the weak coupling expansion of P with numerical values in the case $V = 6^4$. The results are shown in Fig. 12. In the region where the curves are smooth, the error decreases with the order and appears to accumulate. This is very similar to the case of $SU(3)$ [21]. However, it is clear that more reliable estimates for $m \geq 4$ would be desirable for $SU(2)$. It should be noted that for large β the noise in the error is at the same level as the numerical error on P. This would not be the case if we had not included the contribution of the zero mode to b_1 as shown in the second part of Fig. 12.

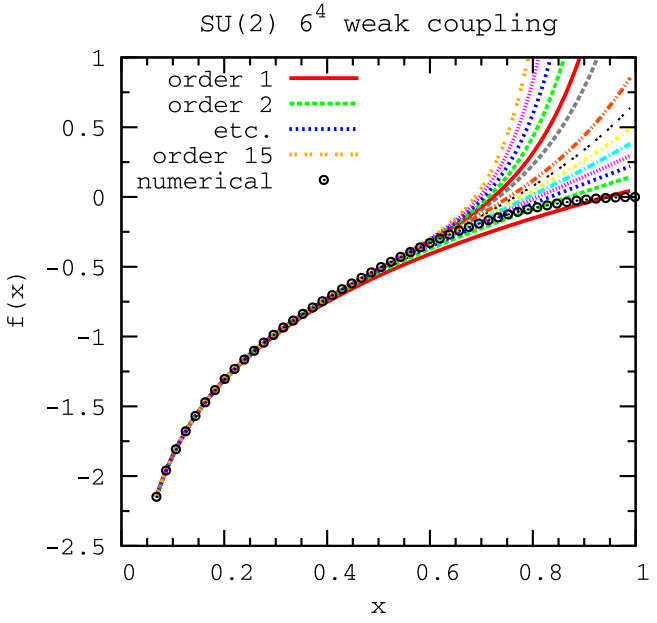

FIG. 13 (color online). Numerical value of $f(x)$ compared to the weak coupling expansion at successive orders.

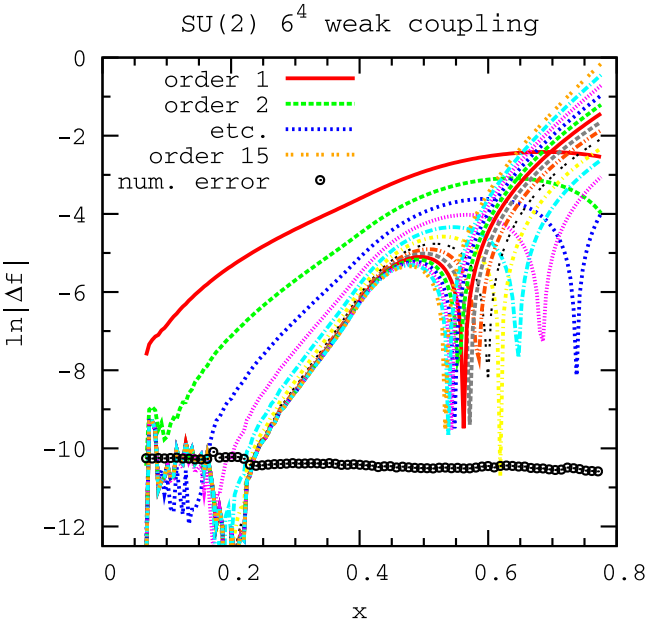

FIG. 14 (color online). Logarithm of the absolute value of the difference between the numerical data and the weak coupling expansion of f at successive orders. For reference, we give the estimated numerical error on f.

We have compared the weak coupling expansion of $f(x)$ with numerical values in the case $V = 6^4$. The results are shown in Fig. 13. The differences are resolved in Fig. 14. In these graphs we have taken $f_0 = -0.146\,63$, which maximizes the length of the accumulation line on the left of Fig. 14.

VII. EXPANSION IN LEGENDRE POLYNOMIALS

We now consider the function $h(y)$, which is $g(y)$ with the logarithmic singularity subtracted as defined in Eq. (17). This is a bell-shaped even function defined on the interval $[-1, 1]$. We can expand this function in terms of the even Legendre polynomials:

$$h(y) = \sum_{m=0} q_{2m} P_{2m}(y). \tag{26}$$

The q_{2m} can be determined from the orthogonality relations with interpolated values of $h(y)$ to perform the integral. A minor technical difficulty is that we do not have numerical data all the way down to $y = -1$. This is because as $y \to -1^+$, or in other words $x \to 0^+$, $\beta \to +\infty$ where the plaquette distribution becomes infinitely narrow. Consequently there is a small gap in the numerical data that needs to be filled. Fortunately, this is precisely where the weak coupling expansion works well. Using the weak coupling expansion (including the overall constant), subtracting $A \ln(x(2-x))$ and shifting to the y coordinate, we obtained the approximate behavior near $y = -1$ for the 6^4 data:

TABLE III. Legendre polynomial coefficients q_{2m} with the three methods described in the text.

Method	4^4 + fit	6^4 + fit	6^4 + (27)
m	q_{2m}	q_{2m}	q_{2m}
0	−0.300 34	−0.300 95	−0.300 96
1	−0.479 63	−0.481 59	−0.481 64
2	0.1488	0.148 53	0.148 45
3	−0.032 15	−0.0309	−0.030 99
4	−0.008 22	−0.008 43	−0.008 52
5	0.011 56	0.011 14	0.011 07
6	−0.003 63	−0.003 05	−0.003 08
7	−0.001 86	−0.001 79	−0.0018
8	0.001 94	0.001 46	0.001 47
9	0.000 08	0.000 26	0.000 28
10	−0.000 94	−0.000 69	−0.000 67

$$h(y) \simeq 0.2145 + 1.2961y + 0.5261y^2 + 0.1109y^3. \quad (27)$$

In order to estimate the error associated with this approximation we have compared with an extrapolation of a quadratic fit of the leftmost part of the data. In order to give an idea of the volume effects, we have also used the second method on a 4^4 lattice. The results are shown in Table III. This indicates that the variations are small and increase with the order in relative magnitude and that the volume effects are stronger than the dependence on the extrapolation procedure. The logarithm of the coefficients is shown in Fig. 15, which illustrates the exponential decay of the coefficients.

The expansion provides excellent approximation of $h(y)$ shown in Fig. 16. The errors are resolved in Fig. 17. It is also possible to calculate $P(\beta)$ by solving the saddle point equation (13) using successive approximations for h. This is shown in Figs. 18 and 19. The spikes in the error graphs correspond to changes of the sign of the errors. It is important to notice that the quality of the approximations improves with the order in all regions of the interval.

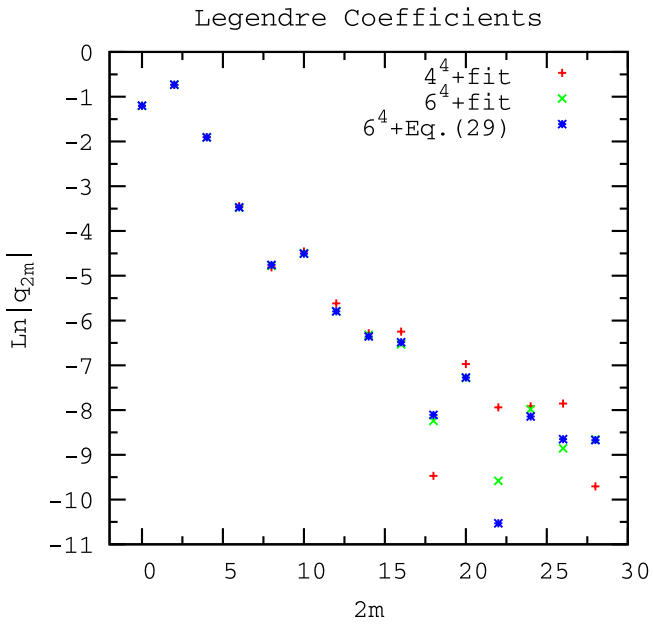

FIG. 15 (color online). Legendre polynomial coefficients q_{2m} with the three methods described in the text.

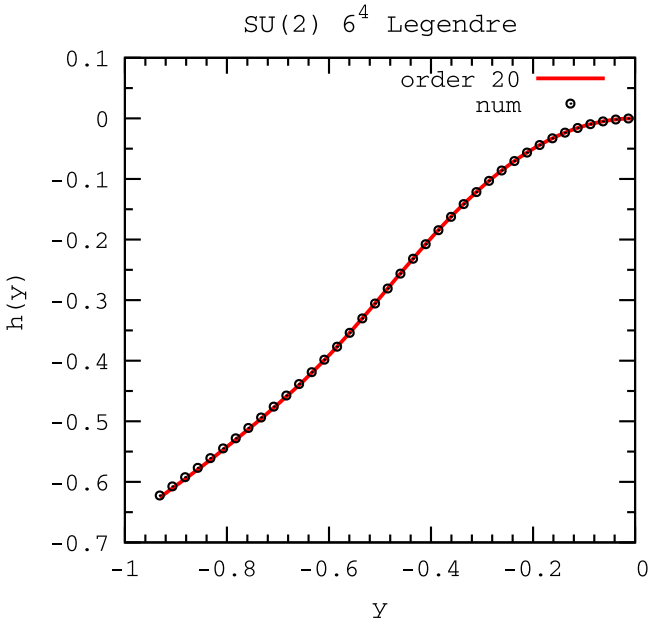

FIG. 16 (color online). $h(y)$ together with the expansion in Legendre polynomials up to order 20.

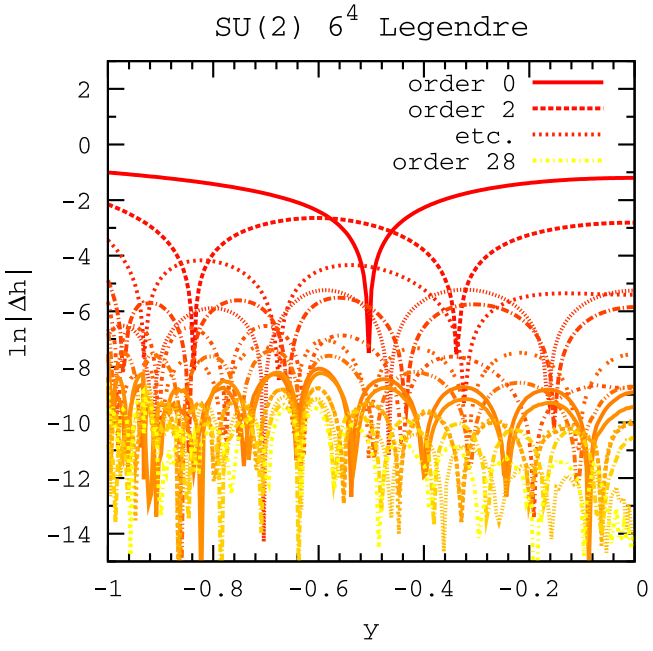

FIG. 17 (color online). Logarithm of the absolute value of the difference between the numerical data for $h(y)$ and expansions in Legendre polynomials at successive orders.

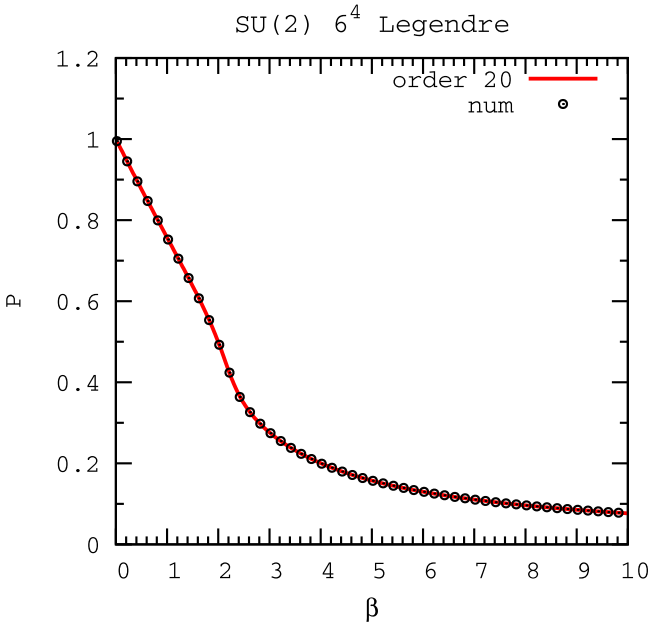

FIG. 18 (color online). P together with the expansion in Legendre polynomials up to order 20.

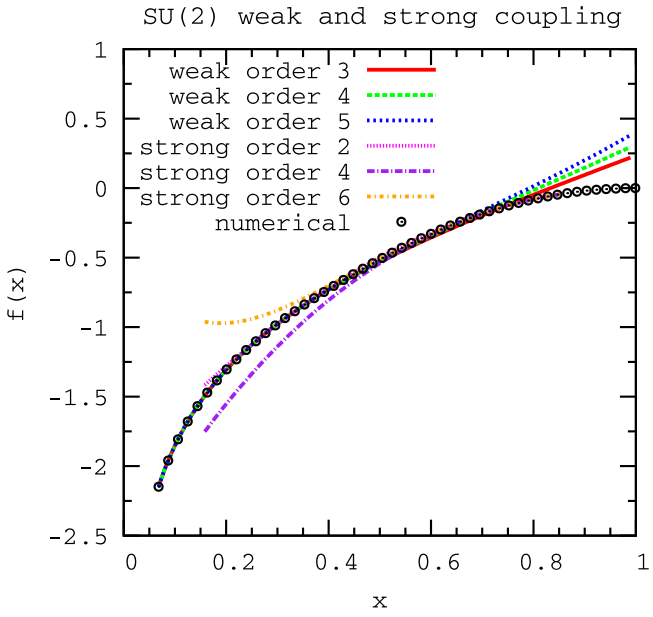

FIG. 20 (color online). Weak and strong coupling expansion of f at a few intermediate orders.

VII. CONCLUSIONS

We have calculated the density of states for $SU(2)$ lattice gauge theory. The intermediate orders in weak and strong coupling agree well in an overlapping region of action values as shown in Fig. 20. However, the large order behaviors of these expansions appear to be similar to the corresponding ones for the plaquette. Volume effects can be resolved well for small action values. Corrections to the saddle point estimate need to be developed systematically. Approximation of a subtracted quantity by Legendre polynomials looks very promising and works well uniformly. We plan to use this approximate form to look for Fisher's zeros. These zeros of the partition function in the complex β plane are important to understand the large order behavior of perturbative series at zero temperature [3] and to check the nature of the finite temperature phase transition.

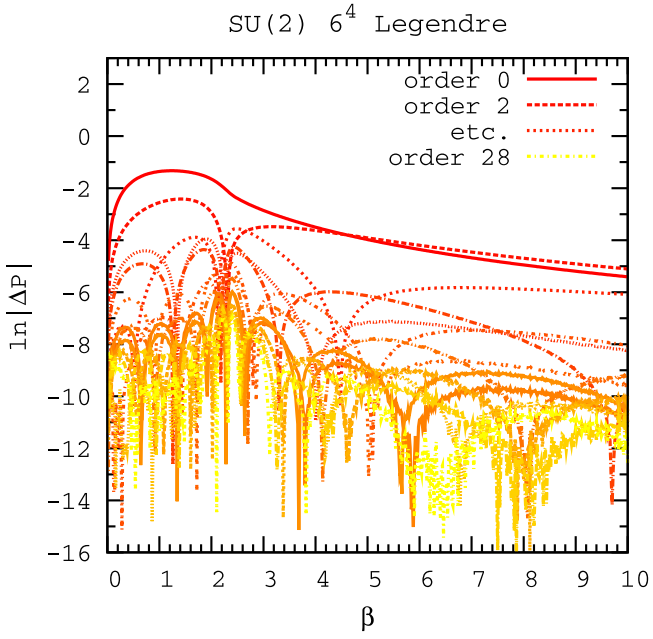

FIG. 19 (color online). Logarithm of the absolute value of the difference between the numerical data for P and expansions in Legendre polynomials at successive orders.

The density of states can be calculated in more general situations. For instance,

$$Z(\beta, \{\beta_i\}) = \int_0^{2\mathcal{N}_p} dS n(S, \{\beta_i\}) e^{-\beta S}, \tag{28}$$

with

$$n(S, \{\beta_i\}) = \tag{29}$$

$$\prod_l \int dU_l \delta\Big(S - \sum_p (1 - (1/N)\mathrm{Re}\,\mathrm{Tr}(U_p))\Big) \tag{30}$$

$$\times e^{-\sum_i \beta_i (1 - \chi_i(U_p)/d_i)}, \tag{31}$$

and χ_i a complete set of $SU(2)$ characters. This is a type of action which naturally arises in the renormalization group studies of $SU(N)$ lattice gauge theories. It is possible to apply exact renormalization group transformation [1,2] or the Monte Carlo renormalization group procedure [22] to the partition function in order to define the couplings. Following the analogy between $f' = \beta$ and $V' = J$ for the effective potential V in the presence of a source J in

scalar models, it would be interesting to study finite size effects from this point of view.

ACKNOWLEDGMENTS

This research was supported in part by the Department of Energy under Contract No. FG02-91ER40664. A. V.'s work was supported by the Joint Theory Institute funded together by Argonne National Laboratory and the University of Chicago and in part by the U.S. Department of Energy, Division of High Energy Physics and Office of Nuclear Physics, under Contract No. DE-AC02-06CH11357.

[1] E. T. Tomboulis, arXiv:0707.2179.
[2] E. T. Tomboulis, Proc. Sci., LAT2007 (2007) 336.
[3] L. Li and Y. Meurice, Phys. Rev. D **73**, 036006 (2006).
[4] J. B. Kogut, Phys. Rep. **67**, 67 (1980).
[5] L. Li and Y. Meurice, Phys. Rev. D **71**, 054509 (2005).
[6] A. Denbleyker, D. Du, Y. Meurice, and A. Velytsky, Proc. Sci., LAT2007 (2007) 269.
[7] N. A. Alves, B. A. Berg, and S. Sanielevici, Phys. Rev. Lett. **64**, 3107 (1990).
[8] A. Denbleyker, D. Du, Y. Meurice, and A. Velytsky, Phys. Rev. D **76**, 116002 (2007).
[9] L. Li and Y. Meurice, Phys. Rev. D **71**, 016008 (2005).
[10] N. A. Alves, B. A. Berg, and R. Villanova, Phys. Rev. B **41**, 383 (1990).
[11] N. A. Alves, B. A. Berg, and S. Sanielevici, Nucl. Phys. **B376**, 218 (1992).
[12] R. Balian, J. M. Drouffe, and C. Itzykson, Phys. Rev. D **11**, 2104 (1975).
[13] R. Balian, J. M. Drouffe, and C. Itzykson, Phys. Rev. D **19**, 2514 (1979).
[14] C. Michael, J. Phys. G **13**, 1001 (1987).
[15] L. Li and Y. Meurice, arXiv:hep-lat/0411020.
[16] U. M. Heller and F. Karsch, Nucl. Phys. **B251**, 254 (1985).
[17] A. Coste, A. Gonzalez-Arroyo, J. Jurkiewicz, and C. P. Korthals Altes, Nucl. Phys. **B262**, 67 (1985).
[18] B. Alles, M. Campostrini, A. Feo, and H. Panagopoulos, Phys. Lett. B **324**, 433 (1994).
[19] F. Di Renzo and L. Scorzato, J. High Energy Phys. 10 (2001) 038.
[20] P. E. L. Rakow, Proc. Sci., LAT2005 (2006) 284.
[21] Y. Meurice, Phys. Rev. D **74**, 096005 (2006).
[22] E. T. Tomboulis and A. Velytsky, Phys. Rev. D **75**, 076002 (2007).